

Application of Quantum-Dressed Classical Mechanics: Molecule Surface Scattering[†]

G. D. Billing

Department of Chemistry, H. C. Ørsted Institute, University of Copenhagen, DK-2100 Ø, Denmark

Received: September 17, 2000; In Final Form: November 8, 2000

Quantum corrections to classical mechanics can be formulated by a new method called quantum-dressed classical mechanics. The method is based on a time-dependent discrete variable representation (DVR) of the wave function. The grid points are defined by the Hermite part of a basis set, the Gauss–Hermite basis set. The formulation introduces a set of grid points which follow the classical trajectory in space. With enough trajectories (DVR points), the method approaches the exact quantum formulation. With just a single grid point in each dimension, we recover classical mechanics. The method is, in the present paper, used to treat the dynamics of molecule surface interaction.

1. Introduction

Quantum corrections to classical mechanics are probably the most fruitful avenue for pursuing the molecular dynamics of large systems. We have recently formulated a new approach to quantum molecular dynamics in which corrections to classical mechanics are easy to introduce. In this manner, we can exploit quantum corrections to ordinary classical trajectory calculations. In our previous applications, the theory has been used for all degrees of freedom in question, i.e., for one degree of freedom (DOF) in a tunneling and a double well problem,¹ in two dimensions for collinear inelastic and reactive scattering,² and in three or four dimensions for an inelastic scattering problem.³ In the present paper, we use the theory to study molecule surface scattering, treating the six degrees of freedom of the molecule by the new approach, whereas the influence of the surface is incorporated by an effective potential in which surface inelastic events as phonon excitation are taken into account. The time-dependent discrete variable representation (DVR) scheme is formally developed by expanding the wave function in a Gauss–Hermite (GH) basis set and then switching to a DVR representation in the solution of the equations for the amplitudes of the GH basis functions. *In this manner, the kinetic operators of the time-dependent Schrödinger equation (TDSE) have already worked on the basis functions and generated classical mechanical equations of motion before the DVR representation is introduced.* The DVR scheme operates with quantum amplitudes for a given grid point rather than with amplitudes for a basis function. Classical mechanics arises naturally as the limit where only one grid point is used for each DOF! The grid points follow the classical dynamics in time and explore the space around the trajectories, thus allowing for quantum delocalization, tunneling, and other quantum phenomena. In the new scheme, the kinetic energy matrix is very simple (*a constant sparse matrix*) which couples the grid point amplitudes within a given mode. In coordinates weighted by the mass and the imaginary part of the width, the kinetic matrix is universal, i.e., independent of the system. All system dependence then appears in the potential coupling matrix, which is even simpler: it is, as in all DVR schemes, diagonal. This is especially important in the present case, where the evaluation of the potential is the

time-consuming part of the calculation. The reason for this is that the dynamics of the molecule are coupled to excitation processes in the solid through a mean field potential, involving a summation over all of the surface atoms and phonon modes in the solid.

Certain ingredients of the method are similar to wave packet propagation:⁴ its extension to GH expansions,^{5–7} the multiconfiguration time-dependent Hartree (MCTDH) approach,⁸ distributed approximating functions (DAF),⁹ ordinary DVR,¹⁰ or time-dependent DVR schemes.¹¹ But, we think that the way these are combined so as to have classical mechanics as the limit of one grid point gives a very compact, flexible, and general approach to molecular dynamics. An approach which could eventually replace both the full classical or full quantum treatment.

Various fragments of method have been presented previously, and the present paper therefore only briefly gives the main ingredients of the method and formulates it for the problem of molecule surface scattering, treating the six degrees of freedom of the molecule by the new approach. The surface phonon coupling is included through an effective potential used in previous work. Finally some numerical calculations on the hydrogen–copper system are discussed.

2. Theory

To illustrate the approach, we consider first a simple one-dimensional case. But, the method can readily be extended to any dimension of interest (see section 3). The theory is as mentioned based upon an expansion of the wave function in the so-called GH basis^{5,6} set, i.e., we have

$$\Psi(x,t) = \sum_n a_n(t) \psi_n(x,t) \quad (1)$$

where $\psi_n(x,t)$ are the GH basis functions

$$\psi_n(x,t) = \pi^{1/4} \exp((i/\hbar)[\gamma(t) + p(t)(x - x(t))] + \text{Re } A(t) [x - x(t)]^2) \phi_n(\xi,t) \quad (2)$$

where

[†] Part of the special issue “Aron Kuppermann Festschrift”.

$$\phi_n(\xi, t) = \frac{1}{\sqrt{n!2^n\sqrt{\pi}}} H_n(\xi) \exp\left(-\frac{1}{2}\xi^2\right) \quad (3)$$

and $\gamma(t)$ determined by normalization $\gamma(t) = -\hbar \ln(2 \operatorname{Im} A(t)/\pi\hbar)/4$. $H_n(x)$ is a Hermite polynomial and

$$\xi = \sqrt{2 \operatorname{Im} A(t)/\hbar} [x - x(t)] \quad (4)$$

We see that the basis set is centered around a trajectory $x(t)$, and the “ground state” $n = 0$ is an ordinary Gaussian wave packet (GWP). The GH basis set has been used previously by several groups,⁷ but the context in which it was used and developed further in refs 5 and 6 is different from those of earlier applications. We think that the development given in this and previous papers on the DVR representation constitute the simplest possible application of this basis set.

The basis set contains, aside from the trajectory $x(t)$, the width parameter $A(t)$ and a momentum parameter $p(t)$. The basis set is orthonormal, i.e.

$$\int dx \psi_n(x, t)^* \psi_m(x, t) = \delta_{nm} \quad (5)$$

if the following relation is used for $\operatorname{Im} \gamma(t)$:

$$\operatorname{Im} \gamma(t) = -\frac{\hbar}{4} \ln(2 \operatorname{Im} A(t)/\pi\hbar) \quad (6)$$

This connection between $\operatorname{Im} \gamma$ and $\operatorname{Im} A$ is compatible with the equations of motion (10 and 11) given below. We now insert the expansion (1) in the TDSE:

$$i\hbar \frac{\partial}{\partial t} \Psi(x, t) = -\frac{\hbar^2}{2m} \frac{\partial^2}{\partial x^2} \Psi(x, t) + V(x) \Psi(x, t) \quad (7)$$

This gives after some manipulations^{5,6} the following set of equations:

$$\dot{x}(t) = p(t)/m \quad (8)$$

$$\dot{p}(t) = -V'_{\text{eff}} \quad (9)$$

$$\dot{A}(t) = -\frac{2}{m} A(t)^2 - \frac{1}{2} V''_{\text{eff}} \quad (10)$$

$$\dot{\gamma}(t) = \frac{p(t)^2}{m} - i\hbar \operatorname{Im} A(t)/m \quad (11)$$

where V'_{eff} and $1/2 V''_{\text{eff}}$ are symbolic expressions for $-\dot{p}(t) - \dot{A}(t) - 2 A(t)^2/m$ respectively. For the expansion coefficients $a_n(t)$, we obtain the following set of equations:

$$i\hbar \dot{a}_n(t) = \sum_k W_{nk} a_k(t) + a_n(t) (E_{\text{kin}} + (2n+1)\hbar \operatorname{Im} A(t)/m) \quad (12)$$

where $E_{\text{kin}} = p(t)^2/2m$ and

$$W_{nk} = \langle \phi_n | V(x) - V(x(t)) - V'_{\text{eff}}(x - x(t)) - (1/2) V''_{\text{eff}}(x - x(t))^2 | \phi_k \rangle \quad (13)$$

i.e., the expansion coefficients are coupled by matrix elements over a potential W which is the actual potential $V(x)$ from which is subtracted the not-yet-defined effective potential expanded to third order around the trajectory $x(t)$. The effective forces V'_{eff} and V''_{eff} have previously been derived by using the Dirac–Frenkel variational theorem.^{5,6} Thus, we obtained⁶

$$V'_{\text{eff}} = \frac{d}{dx} V(x)|_{x=x(t)} + \text{quantum corrections} \quad (14)$$

$$V''_{\text{eff}} = \frac{d^2}{dx^2} V(x)|_{x=x(t)} + \text{quantum corrections} \quad (15)$$

We notice that only in the classical limit the effective forces take the usual form of being a derivative of a potential. Because the solution of the problem is independent of the effective potential (only the convergence pattern in the number of basis functions is affected),¹² the simplest scheme is obtained by propagating the trajectory by using the forces known from classical mechanics, i.e., the “leading” terms in eqs 14 and 15. Thus, we notice that if the potential happens to be of second order the expansion coefficients are not coupled. This is in agreement with the fact that a GWP is the exact solution to the TDSE with a quadratic potential. We see that the present formulation has facilitated the evaluation of the kinetic energy terms and that the coupling matrix is diagonal in what is left of it. Coupling between the expansion coefficients occurs through the potential terms W_{nm} . These potential matrix elements can easily be evaluated if the potential is expanded around the trajectory $x(t)$ in a power series.^{5,6} But, in general, we need to use quadrature or Fourier expansion techniques in order to evaluate the matrix elements. To avoid the computation of matrix elements, we switch to a DVR representation. We notice that this is only possible because the basis set is based on orthogonal polynomials!

2.1. DVR Representation. To obtain the DVR representation, we introduce the grid points as zero's of the N th basis function, i.e., of $\phi_N(z)$. These zero's are those of the N th Hermite polynomial and we introduce

$$a_n(t) = \sum_{i=1}^N c_i(t) \phi_n(z_i) \quad (16)$$

for $n = 0, \dots, N-1$. Here, the index i runs over grid points z_i , and $c_i(t)$ is the amplitude for a given grid point.

The DVR functions are defined as

$$\psi_i(x, t) = \Phi(x, t) \sum_{n=0}^{N-1} \phi_n(z_i) \phi_n(x, t) \quad (17)$$

where

$$\Phi(x, t) = \pi^{1/4} \exp\left(\frac{i}{\hbar}(\gamma(t) + p(t)[x - x(t)] + \operatorname{Re} A(t)[x - x(t)]^2)\right) \quad (18)$$

Equation 23 below could also have been obtained from the TDSE by inserting an expansion of the wave function in the DVR basis functions. It is however easier to use eq 16 and insert this expansion in eq 12.

The DVR functions obey the relation

$$\int dx \psi_i^*(x, t) \psi_j(x, t) = A_i \delta_{ij} \quad (19)$$

or using eq 5

$$\sum_n \phi_n(z_i) \phi_n(z_j) = A_i \delta_{ij} \quad (20)$$

which defines the normalization constant A_i . We notice that the zeros of the N th Hermite polynomial are of course fixed, i.e., $\phi_n(z_i)$ is time-independent. However, in actual space, the grid

points and their position depend on time through the equation

$$x_i = x(t) + \sqrt{\hbar/(2 \operatorname{Im} A(t) z_i)} \quad (21)$$

Thus, the grid points in x space are centered around the trajectory $x(t)$ and spread or contract in time with the magnitude of $\operatorname{Im} A(t)$. However, we notice that a fixed-width approach is obtained by using

$$V''_{\text{eff}} = (4 \operatorname{Im} A(t)^2)/m \quad (22)$$

instead of the derivative of the potential. Thus, with this choice and $\operatorname{Re} A(t=0) = 0$, we get $\operatorname{Im} A(t) = \text{constant}$. To keep the width fixed is advantageous in cases where the (nonlinear) equations of motion for $A(t)$ lead to large values of $\operatorname{Im} A(t)$. We have in the present calculations used the fixed-width approach, and hence if we, for V''_{eff} , use the classical value (the Newton force) the grid points just follow the classical trajectory in space.

Inserting the above expression in the equations (12) we obtain

$$i\hbar \mathbf{A} \dot{\mathbf{c}}(t) = \mathbf{H} \mathbf{c}(t) \quad (23)$$

where \mathbf{A} is a diagonal matrix with elements A_i (see eq 20) and

$$H_{ij} = (E_{\text{kin}} + W(x_i))A_i \delta_{ij} + \frac{\hbar \operatorname{Im} A(t)}{m} \sum_n \phi_n(z_i) (2n+1) \phi_n(z_j) \quad (24)$$

Equation 23 can be brought on a more convenient form by a similarity transformation, i.e.

$$i\hbar \dot{\mathbf{d}}(t) = \mathbf{A}^{-1/2} \mathbf{H} \mathbf{A}^{-1/2} \mathbf{d} \quad (25)$$

where $\mathbf{d} = \mathbf{A}^{-1/2} \mathbf{c}$.

We notice that in the DVR representation the potential is diagonal as usual, and the coupling between the grid points comes about through the last term, which has a very simple time dependence (through $\operatorname{Im} A(t)$). In the fixed-width approach, which is also quite general, also $\operatorname{Im} A(t) = \text{constant}$. This term is what is left of the kinetic energy coupling, but we notice that the kinetic energy operators have already worked on the basis functions. Thus, the “kinetic” coupling elements are time-independent and can be evaluated once and for all. The coupling matrix is furthermore diagonally dominant, which facilitates the solution of eq 25 in a time step. Thus, a Lanczos procedure¹³ iterates to an accurate solution rapidly. Thus, we have¹⁴

$$\mathbf{d}(t + \Delta t) = \mathbf{T} \mathbf{S} \exp\left(-\frac{i}{\hbar} \mathbf{D} \Delta t\right) \mathbf{S}^+ \mathbf{T}^+ \mathbf{d}(t) \quad (26)$$

where \mathbf{T} is an $M \times N$ matrix containing the M recursion vectors, \mathbf{D} a diagonal $M \times M$ matrix, and \mathbf{S} an $M \times M$ matrix which diagonalizes the tridiagonal Lanczos matrix with eigenvalues \mathbf{D} . The number of recursions in each time step Δt depends on the coupling and the accuracy needed. For the problems studied here, 10–15 iterations are needed with $\Delta t = 0.1$ or 0.2 fs. By a simple splitting procedure in which the diagonal part of the kinetic matrix is added to W and the remaining part propagated by a Lanczos method, we may even reduce the number of iterations further in each time step. Thus, we have

$$i\hbar \dot{\mathbf{d}}(t) = (\mathbf{E}(t) + \tilde{\mathbf{A}}) \mathbf{d}(t) \quad (27)$$

where $E_{ii}(t) = W_{ii}(t) + E_{\text{kin}}(t)\delta_{ii} + \tilde{H}_{ii}$ and $\tilde{\mathbf{A}}$ has zeroes in the diagonal, i.e.

$$\tilde{A}_{ii} = 0 \quad (28)$$

$$\tilde{H}_{ij} = \frac{\operatorname{Im} A(t)}{m} \sum_n \phi_n(z_i) (2n+1) \phi_n(z_j) / (A_i A_j)^{1/2} \quad (29)$$

$$\tilde{A}_{ij} = \tilde{H}_{ij} \quad \text{for } i \neq j \quad (30)$$

Because the $\mathbf{E}(t)$ matrix contains the dominating elements we can, by the following splitting

$$\mathbf{d}(t + \Delta t) = \exp\left(-\frac{i}{2\hbar} \mathbf{E} \Delta t\right) \exp\left(-\frac{i}{\hbar} \tilde{\mathbf{A}} \Delta t\right) \exp\left(-\frac{i}{2\hbar} \mathbf{E} \Delta t\right) \mathbf{d}(t) \quad (31)$$

reduce the Lanczos part to propagating the vector $\exp[-i/(2\hbar)\mathbf{E}\Delta t] \mathbf{d}(t)$ with the numerically smaller matrix $\tilde{\mathbf{A}}$. The method is accurate to third order¹⁵ and reduces the CPU requirement by a factor of 2–3 and the number of Lanczos vectors to be stored as well. The method has been tested on three- and four-dimensional (4D) problems.¹⁶ Because the matrix $\tilde{\mathbf{A}}$ is “universal” and, in the fixed-width approach, also constant, further refinements along these lines will certainly be possible.

3. Arbitrarily Sized Systems

We can in a straightforward manner extend the theory to many dimensions d . Introducing the total number of grid points as

$$N = \prod_{i=1}^d N_i \quad (32)$$

where N_i is the number of grid points in dimension i , we have the potential represented at these points as

$$V(x_1^{(1)}, \dots, x_{N_1}^{(1)}, x_1^{(2)}, \dots, x_{N_2}^{(2)}, \dots) \quad (33)$$

The effective potential W is also diagonal in the grid representation and is obtained by subtracting first- and second-derivative terms evaluated at the trajectory $\mathbf{x}(t) = x^{(1)}(t), \dots, x^{(d)}(t)$. Thus, we have

$$W(x_1^{(1)}, \dots, x_{N_d}^{(d)}) = V(x_1^{(1)}, \dots, x_{N_d}^{(d)}) - \sum_{k=1}^d \sum_{i=1}^{N_k} \frac{\partial V}{\partial x^{(k)}} \Big|_{\mathbf{x}(t)} (x_i^{(k)} - x^{(k)}(t)) - \frac{1}{2} \sum_{k=1}^d \sum_{i=1}^{N_k} \frac{\partial^2 V}{\partial x^{(k)2}} \Big|_{\mathbf{x}(t)} (x_i^{(k)} - x^{(k)}(t))^2 \quad (34)$$

The kinetic energy coupling terms are defined by

$$T_{kj}^{(p)} = \prod_{l \neq p} \delta_{i^{(l)} k^{(l)}} \frac{\hbar \operatorname{Im} A_p(t) N_p - 1}{m_p} \sum_{n=0} \phi_n(z_k) (2n+1) \phi_n(z_j) / \sqrt{A_k^{(p)} A_j^{(p)}} \quad (35)$$

for the dimension $p = 1, \dots, d$. N_p is the number of grid points for that mode and k, j are grid points in mode p . The grid points in mode l are denoted $i^{(l)}$. The kinetic energy term couples grid points within a particular coordinate. Thus, the number of nonzero off-diagonal matrix elements of the matrix \mathbf{H} is

$$\prod_{i=1}^d N_i (\sum_{i=1}^d N_i - d) \quad (36)$$

Including the elements in the diagonal we have the total number of nonzero elements as

$$n = \prod_{i=1}^d N_i \sum_{i=1}^d N_i \quad (37)$$

This is then the number of multiplications in each Lanczos iteration. By either storing the index for the elements in the matrix which are nonzero or by careful programming of the kinetic coupling matrix, we can reduce the number of operations to n multiplications. The savings of the method lies in the following important points:

(1) The operation is a simple sparse matrix multiplication, which would vectorize easily on a vector machine.

(2) The number of grid points in dimensions where the dynamics is local is small because the grid points follow the dynamical evolution.

(3) No negative absorbing potentials are needed on the grid.

(4) The dynamics with one grid point is meaningful being the classical limit!

(5) We can add grid points one at a time. Even and odd numbers are allowed.

(6) We can tailor the grid to the dynamical problem.

(7) The method is extremely easy to implement.

Thus, the method provides an easy way of treating some degrees of freedom quantumly while still exploring the classical dynamics of others. This is convenient for large systems where, for instance, the motion of atoms or molecules in solution or clusters conveniently are modeled by traditional molecular dynamics methods. If a given DOF is treated "classically" we have just a single grid point in that mode, i.e., $N_i = 1$. Hence, this mode appears in the dynamical equations only through the classical equations of motion for the trajectory and the effect of the classical value in the potential W .

We notice that the method is extremely simple to program. We need the classical equations of motion eventually together with the equations for the width $A(t)$ for each DOF. A set of grid points for each DOF and the dimension of the coupling matrix is a product of the number of grid points for those DOFs treated quantumly. Because the only thing which needs evaluation in each time step is the potential at each grid point, the amount of storage needed is minimal. When using Lanczos propagating scheme for solving the equations for $d_i(t)$ we usually store the M recursion vectors, i.e., the storage requirement is then $M \times N$. At the expense of extra CPU, we may calculate the recursion vectors twice in each time-step or store the recursion vectors on disk. In either case, the storage requirement in fast memory is reduced to just three recursion vectors, i.e., a total of $3N$. This means that we can handle six-dimensional (6D) quantum calculations on a PC computer with modest memory. However, for large systems, the real advantage of the method comes about if a large part of the system can be treated with just one or two grid points. In any case, the formulation offers a straightforward way of testing whether a classical mechanical description of a given DOF is adequate.

4. An Example

We consider as an example the scattering of a hydrogen molecule from a solid. The molecule has six degrees of freedom,

which may be quantized. The coupling to the solid is modeled through an effective potential of the so-called mean-field type,¹⁷ however, with a detailed balance correction.¹⁷ Thus, the Hamiltonian for the molecule is

$$-\frac{\hbar^2}{2M} \left(\frac{\partial^2}{\partial X^2} + \frac{\partial^2}{\partial Y^2} + \frac{\partial^2}{\partial Z^2} \right) - \frac{\hbar^2}{2m} \left(\frac{\partial^2}{\partial x^2} + \frac{\partial^2}{\partial y^2} + \frac{\partial^2}{\partial z^2} \right) + V_0(x,y,z,X,Y,Z) + V_{\text{eff}}(x,y,z,X,Y,Z,t,T_s) \quad (38)$$

where M and m are the total and reduced mass of the molecule, respectively. We have used the Cartesian coordinates x , y , and z for the molecule vector \mathbf{r} and X , Y , and Z for the center-of-mass position in a coordinate system located at the copper surface such that $Z = 0$ corresponds to the top layer of the copper atoms. The copper crystal is modeled by 130 atoms in three layers, and the coupling to the surface phonons is included through the time and temperature dependence of the effective potential V_{eff} . The surface temperature was taken to be 300 K. The potential surface is constructed by fitting the parameters of an embedded diatomics in molecules model (EDIM) to density functional data. The smallest barrier height is about 40 kJ/mol, and the potential allows by its construction for coupling to the surface phonons. Although 6D calculations with mixed basis set and grid methods have appeared,^{18,19} they have been carried out on a surface excluding the phonon coupling.

For a derivation of the EDIM representation of the molecule surface interaction and effective time and surface temperature-dependent potential, the reader is referred to previous work.¹⁷ Our main concern here is to use the new time-dependent DVR approach on the molecule degrees of freedom. We have performed both 4D and 6D quantum calculations. In the 4D quantum calculations, the number of gridpoints in the X and Y coordinates is just one, i.e., classical mechanics is assumed here. In the 6D quantum calculations, 2–7 gridpoints in these degrees of freedom are included.

In the 4D case, the initial wave function is taken as

$$\Psi(x,y,z,Z,t_0) = \frac{1}{r} g_n(r) Y_{jm}(\theta,\phi) \Phi_{\text{GWP}}(Z,t_0) \quad (39)$$

where r is the bond distance, θ and ϕ are the orientation of the diatomic molecule, $g_n(r)$ is a Morse wave function, Y_{jm} is a spherical harmonics, and Γ_{GWP} is a GWP

$$([2 \text{Im } A_Z(t_0)]/\pi\hbar)^{1/4} \exp\left(\frac{i}{\hbar} P_Z(t_0)[Z - Z(t_0)] - \frac{1}{\hbar} \text{Im } A_Z(t_0)[Z - Z(t_0)]^2\right) \quad (40)$$

which has a momentum distribution¹⁴

$$c(k_0) = \sqrt{2/\pi}\Delta \exp(-2[\Delta(k - k_0)]^2) \quad (41)$$

where $\Delta = 1/2[\hbar/(\text{Im } A_Z(t_0))]^{1/2}$, $\hbar^2 k^2/2M = E - E_{ij}$, and $\hbar^2 k_0^2/2M = E_0 = P_Z(t_0)^2/2M$.

In 6D, also the X and Y coordinates are initialized as GWPs with width parameters $\text{Im } A_X(t_0) = \text{Im } A_Y(t_0)$ and $\text{Re } A_X(t_0) = \text{Re } A_Y(t_0) = \text{Re } A_Z(t_0) = 0$. The initial wave function is projected on the grid basis using that

$$x = r \sin \theta \cos \phi \quad (42)$$

$$y = r \sin \theta \sin \phi \quad (43)$$

$$z = r \cos \theta \quad (44)$$

TABLE 1: Representation of the Initial Vibrational–Rotational States $n,j,m = 0,0,0$ and $1,10,0$ for Various Choices of the Width $\text{Im } A_x(t_0) = \text{Im } A_y(t_0) = \text{Im } A_z(t_0)$ and Grid Points $n_4 = n_5 = n_6^a$

n_4	$n,j,m = 0,0,0$				$n,j,m = 1,10,0$
	$\text{Im } A_x(t_0) = 0.16$	$\text{Im } A_x(t_0) = 0.20$	$\text{Im } A_x(t_0) = 0.25$	$\text{Im } A_x(t_0) = 0.30$	$\text{Im } A_x(t_0) = 0.25$
10	0.946	1.075	0.951	0.856	0.754
12	1.039	0.988	1.017	0.964	0.880
14	1.004	1.003	0.992	1.021	1.012
16	1.012	0.987	1.006	0.996	0.963
18	0.986	1.007	0.999	0.999	0.919
20	0.995	0.999	1.001	1.000	0.936
21	0.998	1.000	1.002	0.998	1.022

^a The width is in units of amu/τ , where $\tau = 10^{-14}$ s.

TABLE 2: Energy- and State-Resolved Probabilities for Inelastic Scattering of Hydrogen from a Copper Surface Obtained by Propagating a Single Wavepacket with a DVR Grid (1,1, n_3 ,20,20,20)^a

energy	n_3	(0,0)	(0,2)	(0,4)	(0,6)	(1,0)	P_{stick}
90 kJ/mol	15	0.41	0.46	0.040	0.0	0.0005	0.075
	16	0.43	0.47	0.047	0.0	0.0003	0.040
	17	0.43	0.47	0.053	0.0	0.001	0.051
100 kJ/mol	15	0.25	0.32	0.033	0.0	0.0008	0.40
	16	0.25	0.32	0.034	0.0	0.0008	0.40
	17	0.26	0.31	0.033	0.0	0.0007	0.40
110 kJ/mol	15	0.053	0.081	0.073	0.0	0.0018	0.79
	16	0.041	0.073	0.073	0.0	0.0018	0.81
	17	0.038	0.070	0.073	0.0	0.0018	0.82
120 kJ/mol	15	0.001	0.015	0.075	0.001	0.002	0.90
	16	0.005	0.022	0.076	0.001	0.003	0.89
	17	0.010	0.027	0.078	0.001	0.004	0.88

^a The kinetic energy E_0 is 100 kJ/mol, and the classical trajectory of the molecule approaches the surface perpendicular at a random site in the unit cell. The projection on the final molecular states and total energies is carried out using the expression given in the Appendix. The initial vibrational–rotational state is $(n,j) = (0,0)$. The sticking probability is defined as $P_{\text{stick}} = 1 - \sum_{n',j'} P_{n',j'}$.

In this manner, the initial values of the d_i amplitudes are obtained. The number of grid points in the x , y , and z coordinates was taken as 21, giving a good representation of the initial vibrational–rotational state of the hydrogen molecule (see Table 1). The average probabilities for inelastic scattering are obtained by projection of the wave function in the grid representation on vibrational–rotational states after the molecule has been scattered from the surface, without energy resolving the initial translational wave packet. However, because the initial wave packet in the translational motion is a GWP it has a width also in momentum space, making it possible to get energy-resolved probabilities out of the calculation by projection on outgoing plane waves in the Z coordinate (see the expression in the Appendix). We have in Table 2 shown the result of calculations with enough grid points in the Z coordinates for projection on a range of total energies. The table shows that 15–17 grid points are sufficient for energy- and state-resolved probabilities. The numbers for sticking obtained with the present surface are smaller at low energies and probably too large at higher energies as compared with those of the experimental data.²⁰ Note that the sticking probability is defined as a sum of the dissociation and the adsorption probability. The latter process is important but only present in calculations including the phonon coupling.²¹ Below we determine the dissociation probability. It turns out to be somewhat smaller than the sticking probability. This is in agreement with our previous findings using classical mechanics for the motion of the molecule. If we are interested in the average reaction probability we simply sum over the amplitudes

TABLE 3: Average Probabilities for Rotational–Vibrational Excitation as a Function of a DVR Basis Set^a

basis/ n',j'	0,0	0,2	0,4	1,(0,2,4)
1,1,3,21,21,21	0.675	0.286	0.020	0.0011
1,1,5,21,21,21	0.633	0.304	0.039	0.0014
1,1,7,21,21,21	0.604	0.327	0.045	0.0014
1,1,3,21,21,21	0.679	0.280	0.022	0.0011
1,1,5,21,21,21	0.625	0.311	0.040	0.0013
1,1,7,21,21,21	0.606	0.317	0.053	0.0015

^a $E_{\text{kin}} = 0.30 \hat{\epsilon}$, and the initial vibrational–rotational state is $n,j = 0,0$. The numbers are averaged over 10 trajectories with random “aiming point” $(X(t_0), Y(t_0))$. Numbers in the upper part of the table include the phonon coupling. $1 \hat{\epsilon} = 100$ kJ/mol.

for grid points having the bond distance r larger than a critical value r^* , i.e.

$$P_{\text{diss}} = \sum_{p=1}^{N_d} |d_p|^2 h(r_p - r^*) \quad (45)$$

where $h(x)$ is a Heaviside function being unity for positive and zero for negative arguments. The value of r_p is obtained as

$$r_p = \sqrt{x_i^2 + y_j^2 + z_l^2} \quad (46)$$

where i, j , and l run over the grid points in the three coordinates. The critical distance for bond breaking is as in previous calculations taken as $r^* = 2.5 \text{ \AA}$. The sticking probability includes also the adsorption process, i.e., $P_{\text{stick}} = P_{\text{diss}} + P_{\text{ads}}$.

Table 3 shows average probabilities obtained using $\text{Im } A_X = \text{Im } A_Y = \text{Im } A_Z = 2 \text{ amu } \tau^{-1}$ and one grid point in the X and Y coordinates. Thus, these are described by classical mechanics. The aiming point, i.e., $X(t_0)$ and $Y(t_0)$, at the surface is chosen randomly, and an average over 10 trajectories is given. To investigate the sensitivity to the number of grid points in Z , we have used the same 10 trajectories in each run. The table shows a modest influence of the phonon coupling, but the phonon coupling has nevertheless been included in all of the calculations except those in the lower half of Table 3. At higher impact energies our previous calculations have shown that the influence of this coupling increases.²²

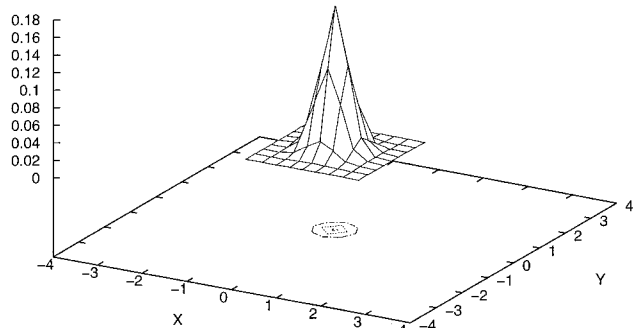
To resolve the rotational–vibrational state of the scattered hydrogen molecule we need as demonstrated in ref 3 about 20 grid points in each coordinate x , y , and z . Energy resolution in the Z -translational motion requires more than the 3–7 grid points included in these calculations. We have therefore reported the “average” probabilities rather than the energy resolved (see the Appendix).

At 50 kJ/mol, we have a possibility for overcoming the barrier for sticking leading to dissociation or trapping at the surface because of coupling to the substrate excitations, a process which

TABLE 4: Average Probabilities for Rotational–Vibrational Excitation of H₂ Colliding with a Cu(100) Surface as a Function of a DVR Basis Set^a

basis/ n',j'	0,0	0,2	0,4	0,6	1,(0,2,4,6)	$P_{\text{ads}} + P_{\text{diss}}$
2,2,3,21,21,21	0.411	0.171	0.118	0.046	0.016	0.226
2,2,5,21,21,21	0.429	0.164	0.106	0.041	0.017	0.229

^a $E_{\text{kin}} = 0.50 \text{ eV}$ and the initial vibrational–rotational state is 0,0. $1 \text{ eV} = 100 \text{ kJ/mol}$.

**Figure 1.** Initial value of the grid probabilities $|d_{ij}|^2$ evaluated at the grid points in a 9×9 grid over the top site of a copper atom. The initial wave function in the X and Y coordinates is a product of two Gaussians.

we shall denote adsorption. Therefore, the probabilities for projection on the hydrogen molecular states do not add up to unity, as is the case at 30 kJ/mol kinetic energy (see Table 4). The number for $P_{\text{ads}} + P_{\text{diss}}$ is in reasonable agreement with that of about 0.3 obtained in ref 21 using classical trajectories.

We can investigate the surface reactivity by reporting the value of $P_r(X,Y)$ evaluated at the grid points in the X and Y coordinates. Thus, we define

$$P_r(X_{i_1}, Y_{i_2}) = \frac{\sum_{i_3, i_4, i_5, i_6} h(r - r^*) |d_{\{i_k\}}|^2}{\sum_{i_3, i_4, i_5, i_6} |d_{\{i_k\}}|^2} \quad (47)$$

Figure 1 shows the initial probability distribution, i.e.

$$P_0(X_{i_1}, Y_{i_2}) = \sum_{i_3, i_4, i_5, i_6} |d_{\{i_k\}}|^2 \quad (48)$$

at the DVR grid points in X and Y placed on the top site of the lattice. The initial wave function in these coordinates is taken as a product of two GWPs

$$\Phi_{\text{GWP}}(X, t_0) \Phi_{\text{GWP}}(Y, t_0) \quad (49)$$

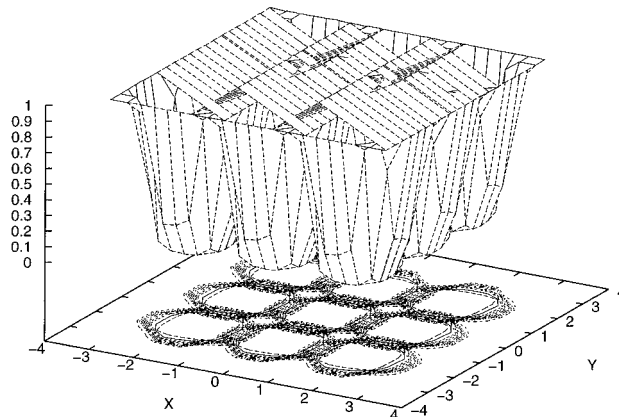
with $\text{Im } A_X(t_0) = \text{Im } A_Y(t_0) = 0.20 \text{ amu}\tau^{-1}$, $X(t_0) = Y(t_0) = 0$, and $P_X(t_0) = P_Y(t_0) = 0$.

With this initial wave function we obtain average reaction probabilities at the kinetic energy 100 kJ/mol. As mentioned above, it is possible to get energy resolution by projecting on the appropriate asymptotic wave functions, which in 6D would be products of diffraction channel and plane wave functions in the X , Y , and Z coordinates (see the Appendix). This projection is possible if the number of gridpoints is increased to about 15 for each dimension. Such calculations are certainly possible within the present framework and will be reported in future work.

Figure 1 gives the initial probability distribution of the wave function in a region from about -1 to $+1 \text{ \AA}$ in the X and Y coordinates. From the scattered wave function, we calculate the same distribution with the constraint that the bond distance

TABLE 5: Average Dissociation Probability over a Unit Cell at $E_{\text{kin}} = 1.0 \text{ eV}$ as a Function of a DVR Basis Set

basis	number of DVR points	P_{diss}
7,7,5,13,13,13	538265	0.128
7,7,5,14,14,14	672280	0.154
9,9,5,13,13,13	889785	0.201
9,9,5,14,14,14	1111320	0.195

**Figure 2.** The site-specific reactivity, i.e., probability for dissociation, at site (X,Y) for a hydrogen molecule with kinetic energy 100 kJ/mol colliding with a Cu(001) surface. The initial state of the molecule is $(n,j) = (0,0)$. A $(9,9,5,14,14,14)$ time-dependent DVR grid was used.

exceeds r^* , and hence, the site specific reactivity can be obtained from the expression.⁴⁷

Four propagations with basis sets ranging from 538 265 to 1 111 320 DVR grid points, respectively, were performed. The average dissociation probability over the unit cell is shown in Table 5. The initial kinetic energy is $E_0 = 100 \text{ kJ/mol}$, the initial rotational–vibrational state is $(0,0)$, and incident angles for the classical trajectory propagating the basis set is $(\theta, \phi) = (0,0)$. Table 5 shows that the numbers obtained with the two largest basis sets are in good agreement, and hence, the site-specific reaction probability can be estimated with sufficient accuracy using about 10^6 grid points. As far as we know, this is the first time that site specificity in the dissociative sticking has been calculated quantum mechanically.²⁴

Figure 2 shows that the probability distribution over the unit cell has a large amplitude for reaction when we get away from the center of the copper atoms located at $X,Y = (0,0)$, $(1.805, 1.805)$, $(-1.805, 1.805)$, etc.

5. Conclusion

We have shown that it is possible to formulate a quantum-dynamical theory in which the grid points follow the classical dynamics of the system. The new approach to quantum molecular dynamics has been used for up to 6D quantum calculations. These calculations have all been carried out on a PC computer.

In this method, we have to integrate Hamilton equations of motion as in ordinary trajectory programs, but in addition, we have a set of equations for the quantum amplitudes $d_i(t)$. The number of grid points influences the size of the time-dependent equations for the \mathbf{d} vector. A classical treatment of the DOF amounts to using only a single grid point. In each time step, we have to evaluate the potential. Because the potential coupling W is diagonal, this process scales as N , the number of grid points. However, the kinetic energy term on the other hand requires no evaluation. It is a constant matrix. Thus, the

numerical effort in the present problem, where the evaluation of the time-dependent coupling matrix is the time-consuming part, scales about linearly with the number of grid points. Another aspect is that absorbing potentials are not needed. Conventional methods usually reserve a large portion of the grid to the wave packet absorption process. For some applications, we furthermore only need the potential in the environment of the classical trajectories. For the present problem, we have previously, by using a conventional grid method, found that about 128–256 grid points in the Z coordinates and 64 or 128 in the r bond coordinate together with say 8–16 in the diffraction coordinates and about 32 grid points for the two rotational angles of the diatomic molecule were necessary. This would amount to about 10^8 – 10^{10} grid points. We have therefore only been able to carry out 4D quantum calculations with conventional methods.²³ By introducing symmetry-adapted basis sets, Kroes et al. were able to reduce the matrix size to about $1-5 \times 10^7$.^{19,25,26} Because we in the present method get the main reduction by using fewer points in Z and r (about 20) we could by combining state expansion techniques with the time-dependent DVR method reduce this number by about 1 order of magnitude. This is important in calculations including phonon coupling, which even with the method used here¹⁷ are about 2 orders of magnitude more time-consuming than calculations without phonons. Also electron–hole-pair excitation may be added to the surface inelastic processes,²¹ and also this is within the possibility of the time-dependent DVR method. If coupling to the surface excitations is included, the time dependence of the interaction potential makes the calculation of the potential the CPU-determining factor, and hence, it is important that this part is linear in the number of grid points.

The method may however be combined with conventional, i.e., state expansion, techniques for some degrees or operator algebraic methods.^{27–29} The number of grid points in a given DOF can be changed according to what property one is interested in. If for instance state-resolved but only average probabilities for inelastic scattering are of interest, we can use one grid point in the coordinates for the center of mass motion (X, Y, Z) but need a relative dense grid in the molecule coordinates. If energy resolution in the energy of the perpendicular motion is needed, we can prepare a wave packet in the Z coordinate, and therefore, more grid points in this DOF are required. If we wish to calculate sticking or reaction probabilities and are not interested in state resolution, we can decrease the number of grid points in (x, y, z) space to about 13–14 in each dimension. Furthermore, we notice that because the grid points follow the trajectory we can let classical mechanics decide upon quantities as branching ratios and project the gridpoints on the channel defined by the trajectory. This possibility is important if the wave function bifurcates. Thus, we do not have to follow the total delocalization at all times but can split the wave function according to the classical dynamics of the system.

Acknowledgment. This research is supported by the Danish Natural Science Research Council and the EU TMR Grant Contract No. HPRN-CT-1999-00005.

Appendix

The energy-resolved and state-resolved probabilities are in the 4D case obtained as a projection of the total wave function on

$$\frac{1}{\sqrt{2\pi}} \exp(ikZ) \frac{1}{r} g_n(r) Y_{jm}(\theta, \phi) \quad (50)$$

which gives

$$P_{n_{jm}}(k) = \frac{k}{k_0} \frac{|c_{n_{jm}}(k)|^2}{c(k_0)} \quad (51)$$

where $c(k_0)$ is the weight of the component k_0 in the initial wave packet and

$$\frac{\hbar^2 k^2}{2M} + E_{n_j} = \frac{\hbar^2 k_0^2}{2M} + E_{n_{j_0}} \quad (52)$$

connects the initial rotational–vibrational energy $E_{n_{j_0}}$ and kinetic energy to the final. The amplitude $c_{n_{jm}}(k)$ is obtained as

$$c_{n_{jm}}(k) = \frac{1}{\sqrt{2\pi}} \frac{\hbar^2}{4} (\text{Im } A_x \text{ Im } A_y \text{ Im } A_z \text{ Im } A_Z)^{-1/4} \sum_{ijkl} \frac{d_{ijkl}}{\sqrt{A_i^{(1)} A_j^{(2)} A_k^{(3)} A_l^{(4)}}} \exp(-ikZ) \frac{1}{r} g_n(r) Y_{jm}(\theta, \phi) \exp \left\{ \frac{i}{\hbar} [p_x(x_i - x(t)) + p_y(t)(y_j - y(t)) + p_z(t)(z_k - z(t)) + P_Z(t)(Z_l - Z(t))] \right\} \exp \left\{ \frac{i}{\hbar} [\text{Re } A_x(x_i - x(t))^2 + \text{Re } A_y(y_j - y(t))^2 + \text{Re } A_z(z_k - z(t))^2 + \text{Re } A_Z(Z_l - Z(t))^2] \right\} \quad (53)$$

Projection in six dimensions on

$$\frac{1}{(2\pi)^{3/2}} \exp[i(k_x X + k_y Y + k_z Z)] \frac{1}{r} g_n(r) Y_{jm}(\theta, \phi) \quad (54)$$

follows a similar expression with a summation over a 6D grid and with an additional factor

$$\frac{\hbar}{2} (\text{Im } A_x \text{ Im } A_y)^{-1/4} \quad (55)$$

and obvious extensions of the expression above.

References and Notes

- (1) Adhikari, S.; Billing, G. D. *J. Chem. Phys.* **2000**, *113*, 1409. Billing, G. D.; Adhikari, S. *Chem. Phys. Lett.* **2000**, *321*, 197.
- (2) Billing, G. D. *J. Chem. Phys.* Submitted for publication; *Int. J. Quantum Chem.* Submitted for publication.
- (3) Billing, G. D. *Chem. Phys.* In press.
- (4) Heller, E. J. *J. Chem. Phys.* **1976**, *63*, 64. Lee, S.-Y.; Heller, E. J. *J. Chem. Phys.* **1982**, *76*, 3035. Huber, D.; Heller, E. J. *J. Chem. Phys.* **1989**, *90*, 7317.
- (5) Billing, G. D. *J. Chem. Phys.* **1997**, *107*, 4286.
- (6) Billing, G. D. *J. Chem. Phys.* **1999**, *111*, 48.
- (7) See, for instance, Coalson, R. D.; Karplus, M. *Chem. Phys. Lett.* **1982**, *90*, 301. Meyer, H.-D. *Chem. Phys.* **1981**, *61*, 335. Kay, K. G. *Phys. Rev. A* **1992**, *46*, 1213.
- (8) Meyer, H.-D. In *The Encyclopedia of Computational Chemistry*; Schleyer, P. von R., Ed.; Wiley: New York, 1998.
- (9) Kouri, D. J.; Ma, X.; Zhu, W.; Petit, B. M.; Hoffman, D. K. *J. Phys. Chem.* **1992**, *96*, 9622.
- (10) See, e.g., Light, J. C.; Hamilton, I. P.; Lill, J. V. *J. Chem. Phys.* **1985**, *82*, 1400.
- (11) Sim, E.; Makri, N. *J. Chem. Phys.* **1995**, *102*, 5615. Manthe, U. *J. Chem. Phys.* **1996**, *105*.
- (12) Billing, G. D. Quantum Classical Methods. In *Lecture Notes*; Lagana, A., Riganelli, A., Eds.; Springer Verlag: Berlin, Germany, 2000.
- (13) See, e.g., Cullum, J. K.; Willoughby, R. A. *Lanczos Algorithms for large Symmetric Eigenvalue Computations*; Birkhäuser: Boston, MA, 1985.
- (14) Billing, G. D.; Mikkelsen, K. V. *Advanced Molecular Dynamics and Chemical Kinetics*; Wiley: New York, 1997.

- (15) See, e.g., DeVries, P. L. *Comput. Phys. Comm.* **1991**, 95, 63.
- (16) Billing, G. D. Unpublished results.
- (17) Billing, G. D. *Dynamics of molecule surface interactions*; Wiley: New York, 2000; *Chem. Phys.* **1982**, 70, 223.
- (18) Gross, A.; Wilke, A.; Scheffler, M. *Phys. Rev. Lett.* **1995**, 75, 2718.
- (19) Kroes, G. J.; Baerends, E. J.; Mowrey, R. C. *Phys. Rev. Lett.* **1997**, 78, 3583.
- (20) Michelsen, H. A.; Auerbach, D. J. *J. Chem. Phys.* **1991**, 94, 7502.
- (21) Billing, G. D. *J. Chem. Phys.* **2000**, 112, 335.
- (22) Billing, G. D. *J. Chem. Phys.* **1993**, 99, 5849.
- (23) Adhikari, S.; Billing, G. D. *J. Chem. Phys.* **2000**, 112, 3884.
- (24) McCormack, D. A.; Kroes, G. J.; Olsen, R. A.; Groeneveld, J. A.; van Stralen, J. N. P.; Baerends, E. J.; Mowrey, R. C. *Chem. Phys. Lett.* **2000**, 317, 328. This paper appeared during the processing of the present manuscript. It reports site- and energy-resolved reactivity on Cu(100) excluding, however, phonon excitations. The results agree qualitatively with our findings on a large reactivity at the bridge and hollow sites. The site specificity is, however, strongly energy-dependent.
- (25) Kroes, G. J.; Baerends, E. J.; Mowrey, R. C. *J. Chem. Phys.* **1997**, 107, 3309.
- (26) Kroes, G. J. *Prog. Surf. Sci.* **1999**, 60, 1.
- (27) Billing, G. D. *Comput. Phys. Comm.* **1984**, 1, 237.
- (28) Billing, G. D. *Int. Rev. Phys. Chem.* **1994**, 13, 309.
- (29) Billing, G. D. In *Encyclopedia of Computational Chemistry*; Schleyer, P. von R., Ed.; Wiley: New York, 1998; p 1587.